

Viscosity calculations from Hadron Resonance Gas model: Finite size effect

Snigdha Ghosh¹, Subhasis Samanta², Sabyasachi Ghosh³,
and Hiranmaya Mishra⁴

¹Indian Institute of Technology Gandhinagar, Palaj, Gandhi nagar 382355, Gujarat, India

²School of Physical Sciences, National Institute of Science Education and Research,
Bhubaneswar, HBNI, Jatni, 752050, India

³Indian Institute of Technology Bhilai, GEC Campus, Sejbahar, Raipur-492015,
Chhattisgarh, India

⁴Theory Division, Physical Research Laboratory, Navrangpura, Ahmedabad 380 009, India

Abstract

We have attempted to review on microscopic calculation of transport coefficients like shear and bulk viscosities in the framework of hadron resonance gas model, where a special attention is explored on the effect of finite system size. The standard expressions of transport coefficients, obtained from relaxation time approximation of kinetic theory or diagrammatic Kubo-type formalism, carry mainly two temperature dependent components - thermodynamical phase space and relaxation time of medium constituent. Owing to quantum effect of finite system size, thermodynamical phase space can be reduced as its momentum distribution will be started from some finite lower momentum cut-off instead of zero momentum. On the other hand, relaxation time of hadrons can also face finite size effect by considering only those relaxation scales, which are lower than the system size. Owing to these phenomenological issues, we have proposed a system size dependent upper bound of transport coefficients for ideal HRG model, whose qualitative technique may also be applicable in other models. This finite size prescription may guide to shorten the broad numerical band, within which earlier estimated values of transport coefficients for hadronic matter are located. It is also suspected that the hadronic matter may not be far from the (nearly) perfect fluid nature like the quark gluon plasma.

1 Introduction

The ratio between shear viscosity (η) and entropy density (s) of any medium is the quantity, which measures the fluidity of the medium. This ratio η/s is roughly equal to the ratio of mean free path to de-Broglie wavelength of medium constituent. Hence, it can never be vanished, as mean free path of any constituent can never be lower than its de-Broglie wavelength. Other way to comment is that quantum fluctuations prevent the existence of perfect fluid in nature and η/s of any fluid should have some lower bound, which is also claimed from the string theory calculation [1].

Interestingly, a small value of η/s , very close to this quantum lower bound, is observed in super hot medium, produced in heavy ion collision experiment like RHIC [2] and LHC [3].

Some other many body systems like cold atoms [4], graphene [5] and in low energy nuclear matter [6] are also observed to have small η/s near to the lower bound. This nearly perfect fluid behavior at different extreme situations has drawn immense attention from scientific communities working on the field of condense matter physics to nuclear physics to string theory.

Present article is interested on fluid properties of hadronic matter, where a special phenomenological attention is taken care on finite size of the system. One can find a long list of Refs. [15, 14, 7, 8, 9, 10, 11, 12, 13, 16, 18, 19, 20, 17, 21, 22, 23, 24, 25, 26] on microscopic calculations of η/s for hadronic matter, where some of them adopted different hadronic models [15, 14, 7, 8, 9, 10, 11, 12, 13, 16, 18, 19, 20, 17, 21, 22] and some have gone through bulk simulations [23, 24, 25, 26]. Their predicted values of η/s reside within a broad numerical band. Similar kind of broad numerical band is also observed for bulk viscosity ζ of hadronic matter, estimated by earlier Refs. [8, 19, 20, 17, 33, 15, 34, 27, 28, 29, 30, 31, 32]. Recently, Refs. [22, 21] have provided a possible prescription to make the band be narrow, when a finite size effect of medium is considered. Though the prescription is quantitatively applicable in hadron resonance gas (HRG) model, adopted in Refs. [22, 21], but a qualitative application of this prescription can always be possible in other hadronic models. Present article is intended to review this prescription by analyzing earlier estimated values of η/s and ζ/s .

Starting with a brief formalism of transport coefficients (2.1) and HRG model (2.2) parts in Sec. (2), we have explored the results of finite system size effect in next Sec. (3), which contain the discussion about a lower momentum cut-off consideration in thermodynamical quantities and its phenomenological aspect [21]. Next Sec. (4) describe the relaxation time of different hadrons, which are classified in two components, discussed in two subsections (4.1) and (4.2). An upper bound is proposed for finite size of system [22]. Considering a special example in Sec. (4.3), we show how an upper momentum cut-off in relaxation scale help to reduce the values of η/s and ζ/s below their upper bound [22]. At the end in Sec. (5), we have concluded.

2 Formalism

2.1 transport coefficients

The proportional constants between thermodynamical forces and fluxes are basically defined as transport coefficients. Here, we will discuss about the two transport coefficients - shear and bulk viscosities, although other transport coefficients like electrical and thermal conductivities may also be very interesting to study. We start with the energy-momentum tensor of a relativistic fluid $T^{\mu\nu}$ which is split into a ideal and an dissipative part as:

$$T^{\mu\nu} = T_0^{\mu\nu} + T_D^{\mu\nu} , \quad (1)$$

where, $T_0^{\mu\nu} = (\epsilon + P)u^\mu u^\nu - P g^{\mu\nu}$, containing energy density ϵ , pressure P , fluid four-velocity u^μ , metric tensor $g^{\mu\nu}$. Ignoring the heat flow part, the dissipation part of energy momentum tensor will be

$$T_D^{\mu\nu} = \eta U_\eta^{\mu\nu} + \zeta U_\zeta^{\mu\nu} \quad (2)$$

where thermodynamical fluxes for shear (η) and bulk (ζ) viscosities are

$$U_\eta^{\mu\nu} = D^\mu u^\nu + D^\nu u^\mu + \frac{2}{3} \Delta^{\mu\nu} \partial_\sigma u^\sigma$$

$$U_\zeta^{\mu\nu} = \Delta^{\mu\nu} (\partial^\alpha u_\alpha) \quad (3)$$

with $D^\mu = \partial^\mu - u^\mu u^\sigma \partial_\sigma$ and $\Delta^{\mu\nu} = g^{\mu\nu} - u^\mu u^\nu$.

Here, we are going to discuss about two different approaches for the evaluation of η and ζ namely: (i) kinetic theory approach and (ii) Kubo approach.

In former approach, we assume that each hadrons in the medium is deviated from their equilibrium distribution function $f_h^0 = 1/[e^{\omega_h/T} + a_h]$ by a small amount $\delta f = \phi f_h^0(1 + a_h f_h^0)$, where $a_h = \pm 1$ for boson and fermion respectively; $\phi = a_\eta k_\mu k_\nu U_\eta^{\mu\nu} + a_\zeta U_\zeta^{\mu\nu}$ is assumed in terms of same tensor decomposition as given in Eq. (2). In terms of these quantities, the dissipative part of energy-momentum tensor,

$$T_D^{\mu\nu} = \sum_h g_h \int \frac{d^3 \vec{k}}{(2\pi)^3} \frac{k^\mu k^\nu}{\omega_h} \delta f, \quad (4)$$

can be obtained in the form of Eq. (2), where the expressions of η and ζ will come in term of unknown coefficients a_η and a_ζ . Now, using the relaxation time approximation of relativistic Boltzmann transport equation,

$$p_h^\mu \partial_\mu f_h(x, p_h) = -p_h^0 \frac{\delta f_h}{\tau_h}, \quad (5)$$

the unknown coefficients a_η , a_ζ can be obtained and we will get RTA expression of η and ζ as [33, 34]

$$\eta = \sum_h \frac{g_h}{15T} \int \frac{d^3 \vec{k}}{(2\pi)^3} \tau_h \left(\frac{\vec{k}^2}{\omega_h} \right)^2 f_h^0 (1 - a_h f_h^0), \quad (6)$$

$$\zeta = \sum_h \frac{g_h}{T} \int \frac{d^3 \vec{k}}{(2\pi)^3 \omega_h^2} \tau_h \left\{ \left(\frac{1}{3} - c_s^2 \right) \vec{k}^2 - c_s^2 m_h^2 \right\}^2 f_h^0 (1 - a_h f_h^0), \quad (7)$$

where c_s is the velocity of sound in the medium and τ_h is relaxation time of h hadron. The g_h is degeneracy factors of hadrons due to spin, isospin (including particle, anti-particle counting as we are interested on zero baryon density picture).

Similar kind of expressions can be obtained in Kubo approach, where transport coefficients are defined as zero energy-momentum limit of correlators, constructed by energy momentum tensor. The standard (field theoretical version) Kubo expressions of η and ζ are [8, 9, 35]

$$\begin{aligned} \eta &= \frac{1}{20} \lim_{q_0, \vec{q} \rightarrow 0} \frac{\int d^4 x e^{iq \cdot x} \langle [\pi^{ij}(x), \pi_{ij}(0)] \rangle_\beta}{q_0}, \\ \zeta &= \frac{1}{2} \lim_{q_0, \vec{q} \rightarrow 0} \frac{\int d^4 x e^{iq \cdot x} \langle [\mathcal{P}(x), \mathcal{P}(0)] \rangle_\beta}{q_0}, \end{aligned} \quad (8)$$

where the operators π_{ij} and \mathcal{P} can be obtained from energy-momentum tensor $T^{\mu\nu}$ as,

$$\begin{aligned} \pi^{ij} &\equiv T^{ij} - g^{ij} T_k^k / 3, \\ \mathcal{P} &\equiv -T_k^k / 3 - c_s^2 T^{00}. \end{aligned} \quad (9)$$

When one builds $T^{\mu\nu}$ from free Lagrangian density, the correlators take the form in terms of boson or fermion fields and then we will get a simplest one-loop skeleton level diagram,

which is divergent in zero energy-momentum limit. To cure this divergence, a finite thermal width ($\Gamma_h = 1/\tau_h$) is generally introduced in the propagators of one-loop diagram and at the end of the calculation [8, 9, 35], we will get same expressions of η and ζ , as obtained in RTA method, given in Eqs (6), (7).

2.2 Thermodynamical quantities from HRG model

In this work, we aim to calculate the quantities η/s and ζ/s from Eqs. 6 and 7 for which the necessary inputs are the thermodynamic quantities: entropy density s and speed of sound c_s of the medium. A unified thermodynamics of quark and hadronic matter with a smooth cross-over quark-hadron transition can be obtained from lattice QCD simulations [37, 38]. It is remarkable that, QCD thermodynamics in the low temperature region ($100 < T < 160$) MeV can be achieved analytically by considering a grand canonical ensemble of all the non-interacting hadrons- a formalism known as Hadron Resonance Gas (HRG) Model [36]. We start with the grand canonical partition function at zero chemical potential ($\mu = 0$)

$$\ln \mathcal{Z}(T, V, \mu = 0) = V \int \frac{d^3p}{(2\pi)^3} \sum_h g_h a_h \times \ln [1 + a_h \exp \{-\beta \omega_h\}] . \quad (10)$$

All the relevant thermodynamic quantities like pressure (P), energy density (ε), entropy density (s) and speed of sound (c_s) are obtained from the partition function as:

$$s = \left(\frac{\varepsilon + P}{T} \right) = \frac{1}{T} \left\{ \left(\frac{T}{V} \right) \ln \mathcal{Z} + \left(\frac{T^2}{V} \right) \frac{\partial}{\partial T} (\ln \mathcal{Z}) \right\} \quad (11)$$

$$c_s^2 = \left(\frac{\partial p}{\partial \epsilon} \right) = \left(\frac{\partial p}{\partial T} \right) / \left(\frac{\partial \epsilon}{\partial T} \right) . \quad (12)$$

Now, using the Eq. (10) in Eqs. (11) and (12), one can obtain s and c_s^2 , which is presented by red solid line in Fig. 1(a) and (b) respectively. The entropy density has been normalized by its Stefan-Boltzmann (SB) limit $s_{SB} = \frac{19\pi^2}{9} T^3$ (for 3 flavor quarks). The LQCD data of s/s_{SB} and c_s^2 from the WB group [37] (triangles) and Hot QCD group [38] (circles) are also plotted in Fig. 1(a) and (b), which are in well agreement with the red solid curves, obtained in ideal HRG model. This friendship between HRG model and LQCD within the hadronic temperature range is well familiar fact.

3 Finite size: Lower momentum cut-off

Here we want to shift our focus on some phenomenological point, where we will consider that the hadronic medium, produced in heavy ion collision experiments, has some finite size. So idea is to modify the theoretical tools of (ideal) HRG model for applying in realistic scenario, where the hadronic matter carry a finite size.

Reader can find a vast literature [39, 40, 41, 42, 43, 44, 45, 46, 47, 48, 49, 50, 51] on finite size method, where we will consider the simplest toy model, as adopted in Refs. [46, 47, 51]. If the volume is so small that the quantum effect can not be ignored then one can roughly relate the system with the quantum mechanical picture for particle in a box. Hence, the lowest possible zero momentum in classical picture will be transformed to a finite value in quantum picture, which depends on the size as [46, 47, 51]

$$k_{\min} = \pi/R , \quad (13)$$

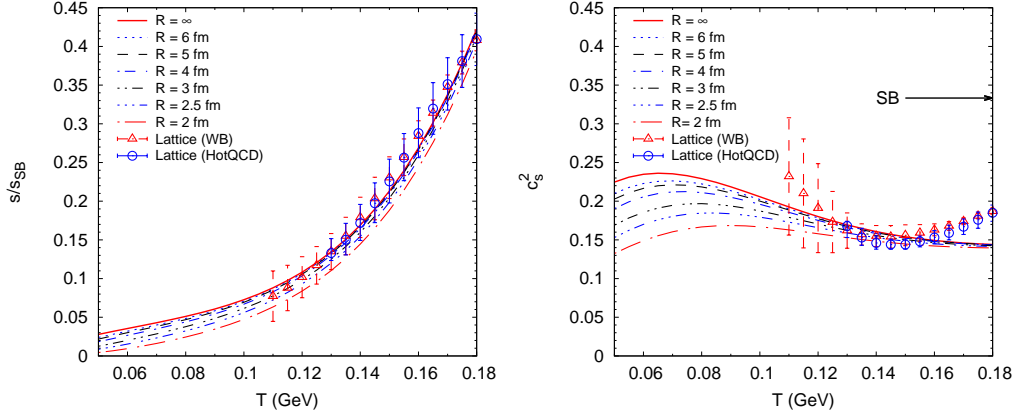


Figure 1: (Color online) (a) The ratio of entropy density to its Stefan-Boltzmann (SB) value (s/s_{SB}) is plotted against T for different values of R . (b) Square of speed of sound (c_s^2) versus T for different values of R . The Stefan-Boltzmann limit of c_s^2 is shown by the arrow. Corresponding LQCD data from the WB group [37] (triangles) and Hot QCD group [38] (circles) are also shown.

where R is the size of a cubic volume $V \sim R^3$ of the system. Let us call it lower momentum cut-off. So, implementing the transformation

$$\int_0^\infty \rightarrow \int_{k_{\min}}^\infty \quad (14)$$

in Eq. (10), one can get a partition function of finite size hadronic matter. In principle, the integration should also be converted to sum over discrete momentum values but for simplicity we have not considered that. This simplified approximated picture is well justified in Refs. [49, 50]. We have taken six different sizes of $R = 2, 2.5, 3, 4, 5, 6$ fm, whose range is guided from the experimental values, provided in Ref. [52]. In Figs. 1(a-b), we notice that s and c_s^2 both are decreasing as R decreases. It indicates that the values of s and c_s^2 for theoretically assumed infinite hadronic matter can not be considered for experimentally produced medium, having a finite size.

3.1 Phenomenological aspect of lower momentum cut-off

We have noticed that thermodynamical quantities like s , c_s^2 are changed due to lower momentum cut-off (k_{\min}) consideration, mapping the finite size effect. Similarly, shear and bulk viscosities will also be changed, when one transforms the lower limit of integration in Eqs. (6) and (7) from 0 to k_{\min} . The detail result have been addressed in Ref. [21]. Interestingly, we get a link between this microscopic estimation of viscosities for finite size system and the macroscopic evolution picture. For non-central collision, the freeze-out size R becomes smaller. So one can expect different values of transport coefficients for different centrality, which is mapped by the number of participant N_{part} . From the table 8 of Ref [52] for Au+Au collision at RHIC energy $\sqrt{s_{NN}} = 200$ GeV, we have taken the experimental data of centrality or N_{part} dependence of chemical freeze-out parameters such as temperature T , chemical potential μ_B and system size R . After parameterizing the data,

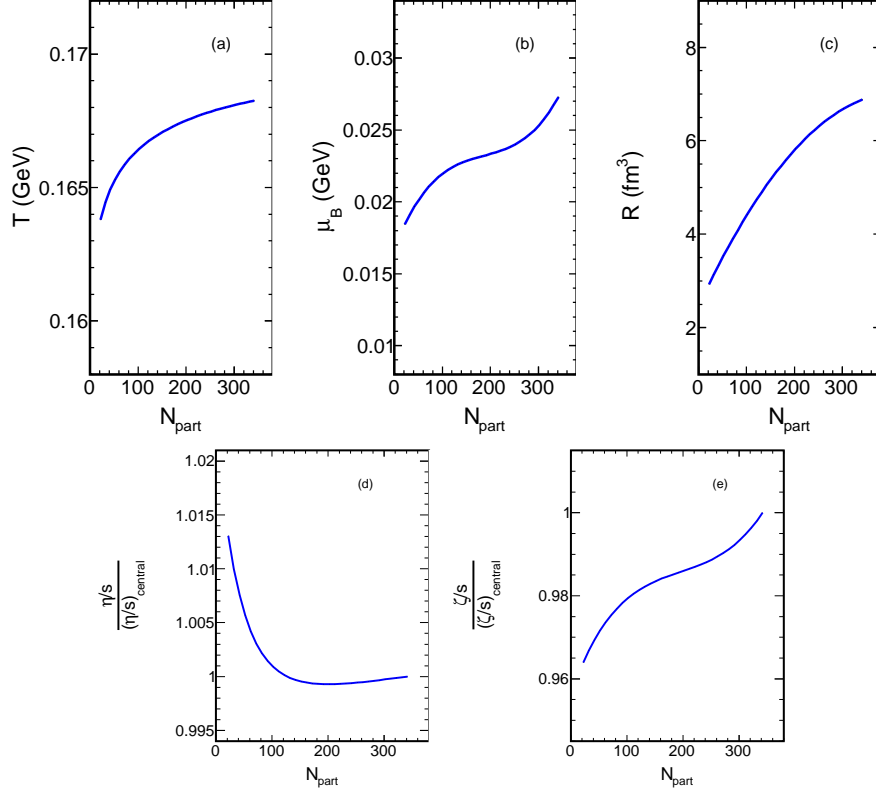


Figure 2: N_{part} dependence of temperature T (a), baryon chemical potential μ_B (b) and radius R (c) of the medium at freeze-out point, taken from Ref. [52]. Using those inputs, the dimensionless transport coefficients η/s (d), ζ/s (e) are plotted against N_{part} .

the functions $T(N_{\text{part}})$, $\mu_B(N_{\text{part}})$ and $R(N_{\text{part}})$ are plotted in Figs. 2(a)-(c), which shows roughly the variation $R = 7 - 3$ fm, $\mu_B = 0.027 - 0.019$ GeV and $T = 0.168 - 0.164$ GeV for $N_{\text{part}} = 350 - 40$. So R faces major changes and T , μ_B face mild changes due to change of N_{part} . Using those input values of T , μ_B and R in Eqs. (6) (7) and (11), we have obtained corresponding N_{part} dependence of η/s and ζ/s , where R enters in the lower limit of integration by following Eqs. (13), (14). These η/s and ζ/s are plotted against N_{part} in Figs. 2(d) and (e), where their values have been normalized by the corresponding values at most central collision, carrying maximum N_{part} . We notice that η/s decreases with N_{part} . Interestingly, similar trend is expected from hydrodynamical simulation [53], where η/s is entered as an input parameter. This qualitative agreement between microscopic [21] and macroscopic [53] investigations is pointing out the importance of size-dependent transport coefficient calculations.

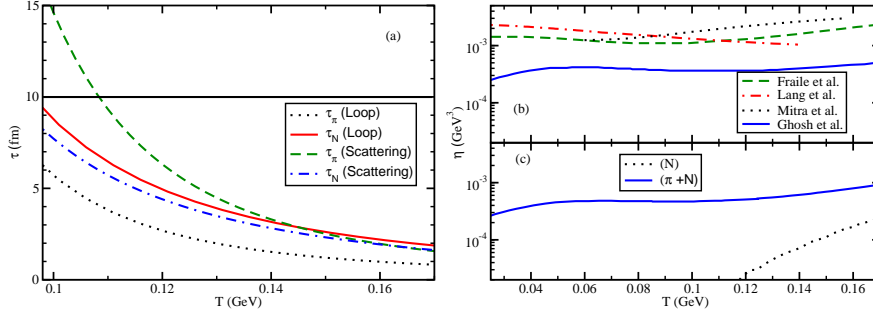


Figure 3: (Color online) (a) Dotted and dash lines respectively denote the pion relaxation time τ_π from loop [11] and scattering [10] diagrams calculations; Same for nucleon relaxation time τ_N are displayed by solid [12] and dash-dotted [13] lines respectively. (b) Shear viscosities of pion, obtained by Fraile et al. [8], Lang et al. [9], Mitra et al. [10], Ghosh et al. [11]. (c) Contribution of nucleon (dotted line) and (pion + nucleon) (solid line) from Ref. [12].

4 Relaxation time

So far we have concentrated on thermodynamical phase space parts of η and ζ expressions, given in Eqs. (6), (7). The known values of different hadron masses [54] fix its numerical strength. Beside this thermodynamical phase space part, another part is relaxation time τ_h , which will be analyzed in this section.

Based on the phenomenological picture of dissipation, hadrons may be classified into two categories - non-resonance (\mathcal{NR}) and resonance (\mathcal{R}) components.

4.1 Non-Resonance (\mathcal{NR}) component

Let us first discuss about \mathcal{NR} component, then we will come to the discussion of \mathcal{R} component in next subsection.

Long lived particles like pseudo-scalar meson nonet and baryon octet may be considered as \mathcal{NR} members as they can't decay within the life time of the fireball, produced in HIC experiments. For simplicity, we considering only pion, kaon and nucleon as \mathcal{NR} members as they are most abundant constituents in the medium. They participate in dissipation via their strong interaction scattering process. Due to their dominant contribution in dissipation, many of the earlier works have focus on pion gas [7, 8, 9, 10, 11] and (pion + nucleon) [12, 13, 14] gas instead of going to all hadrons, as considered in HRG model [16, 17, 18, 19, 20]. Relaxation time (τ_π) or length (λ_π) of pion, obtained from π^4 -type interaction Lagrangian density, has been considered by Lang et al. [9]. Based on the optical theorem of thermal field theory, they have derived the thermal width of pion $\Gamma_\pi = 1/\tau_\pi$ from the imaginary part of pion self-energy diagram, containing two-loop with 3 pion propagators. Using the temperature and momentum dependent relaxation time of pion in Eq. 6, they have estimated temperature dependent shear viscosity of pion (η_π), which is shown by red dash-dotted line in Fig. 3(b). This leading order interaction Lagrangian density from Chiral Perturbation Theory (ChPT) can only describe the pion interaction but can't generate the resonances ρ and σ mesons, as experimentally observed in $\pi\pi$ scattering cross section. These resonances ρ

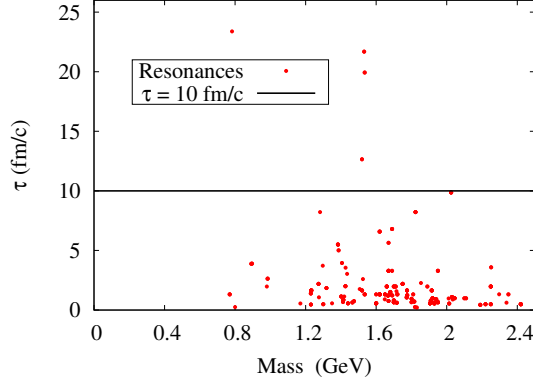


Figure 4: (Color online) The values of mean life times (red points) for different hadron *resonances* up to 2.5 GeV masses. The horizontal line indicates an approximated life time of the hadronic medium, produced in heavy ion experiments.

and σ mesons can be introduced via phenomenological $\sigma\pi\pi$ and $\rho\pi\pi$ interaction Lagrangian densities, as considered in Refs. [11, 10]. Similar resonance picture can also be dynamically generated via unitarization technique, as adopted in Ref. [8]. Shear viscosities of pion in resonance picture of Refs. [8, 10, 11] have been shown by green dash, black dotted and solid blue lines respectively in Fig. 3. Comparing these curves with red dash-dotted lines, we notice that decreasing trend of $\eta_\pi(T)$ in ChPT can be transformed to increasing nature when one introduces the resonances. This is also checked in the Ref. [8]. Now let us come to other \mathcal{NR} member - nucleon. Shear viscosities of nucleon η_N has been calculated in Ref. [12] via phenomenological $N\pi B$ interaction Lagrangian densities, where B stand for different spin 1/2 and 3/2 baryons. The black dotted line and blue solid lines in Fig. 3(c) are respectively displaying the results of η_N and $(\eta_N + \eta_\pi)$ of Ref. [12]. Refs. [11, 12] have obtained the relaxation times τ_π and τ_N from the pion and nucleon self-energies, where $\pi\sigma$, $\pi\rho$ [11] and different NB loops are considered for former case, while latter one carries different πB loops [12], displayed by black dotted and solid red lines in Fig. 3(a). Same quantities τ_π and τ_N in Ref. [10, 13], shown by dash and dash-dotted lines in Fig. 3(a), have been obtained from elastic scattering processes $\pi\pi \rightarrow \pi\pi$, $\pi N \rightarrow \pi N$ and $NN \rightarrow NN$, whose relaxation time scales are $\tau_{\pi\pi}$, $\tau_{\pi N}$ and τ_{NN} . Their mixing relations are $\frac{1}{\tau_\pi} = \frac{1}{\tau_{\pi\pi}} + \frac{1}{\tau_{\pi N}}$, $\frac{1}{\tau_N} = \frac{1}{\tau_{NN}} + \frac{1}{\tau_{N\pi}}$. The straight horizontal line at 10 fm is assumed as maximum possible dimension of hadronic matter and we see that the values of τ_π and τ_N , obtained from both loop and scattering diagrams, are lower than the system size as expected in dissipative fluid picture.

4.2 Resonance (\mathcal{R}) component and total ($\mathcal{NR} + \mathcal{R}$)

Excluding the pseudo-scalar meson nonet and baryon octet, the remaining part of hadronic zoo may be considered as \mathcal{R} members. The mean life times of \mathcal{R} [54] upto $M = 2.5$ GeV are shown by red dots in Fig. 4, where a horizontal line indicates the life time of fireball, which we have roughly considered as 10 fm. The message of the plot is that the \mathcal{R} particles, having mean life times, less than the life time of medium, can only participate in the dissipation

as they only can decay inside the medium. Taking only those \mathcal{R} 's and using their mean life times as the relaxation times τ in Eqs. (6) and (7), we get the contribution of shear and bulk viscosities from \mathcal{R} component.

Now, life time (maximum size) of fireball can be considered as upper limit of relaxation times (relaxation lengths) of \mathcal{NR} particles and after adding this contribution with \mathcal{R} part contribution, we get an upper limit estimation of η and ζ , as shown by pink dotted line in Figs. 5(a) and 6(a).

Normalizing the upper limit estimation of η and ζ by the entropy density s , we get a upper bound for η/s and ζ/s , as shown by pink dotted line in Figs. 5(b) and 6(b). Here,

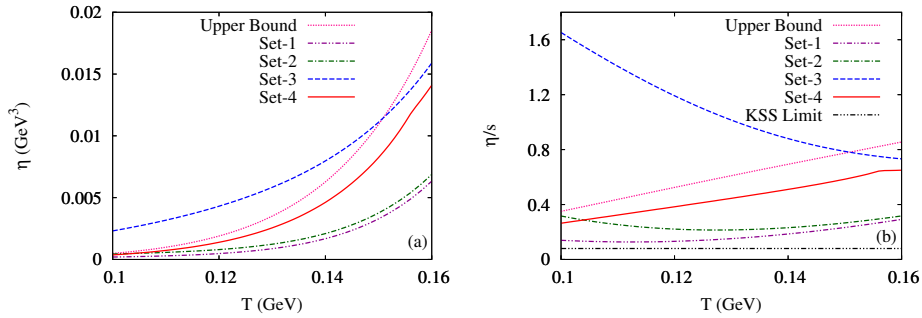


Figure 5: (Color online) (a) Shear viscosity (η) (b) shear viscosity to entropy density ratio (η/s) as a function of temperature for Set-1, 2, 3 and 4, as given in Table (2). An upper bound of both are shown by dotted and the dash-triple-dotted line indicates the KSS limit for η/s .

we see that upper limit estimations for η/s at $T = 0.100$ GeV to 0.160 GeV are around 0.4 to 0.85 , which is not very far from the KSS [1] or quantum lower bound ($\frac{\eta}{s} = \frac{1}{4\pi} \approx 0.08$). It means that a strongly coupled liquid behavior, which is experimentally expected in quark gluon plasma, is quite possible to see also in hadronic matter. The estimated values of η/s at $T = 0.100$ GeV to 0.160 GeV in earlier Refs. [8, 9, 14, 18, 19, 23, 26] are tabulated in Table (1), which also contain the values of ζ/s .

We notice that the values of η/s and ζ/s near transition temperature or at $T = 0.160$ GeV remain approximately within the upper bound, estimated in HRG model for 10 fm system size but it is not true for lower temperature, say $T = 0.100$ GeV. Though upper bound of HRG model should not be considered as reference level of other model-calculations, but their low temperature results may be modified if we properly impose the condition - the relaxation length of medium constituents should not be greater the system size. Refs. [8, 9, 14] and Refs. [23, 26] may not be relevant to compare quantitatively with values of upper bound because former references don't consider \mathcal{R} members and latter references have adopted models other than HRG. So, a direct quantitative comparison can be done with HRG based works - Refs. [18, 19] where both have considered an approximate hard sphere scattering strengths for all hadrons. This equal footing consideration for all hadrons are taken for simplification but one should filter out the resonances, whose interaction time scales are larger than the life-time of the system (~ 10 fm). Using this filtration for \mathcal{R} members, as done in Ref. [22] and using the relaxation time pion and nucleon from Refs. [11, 12], we have create a new set of estimation, which is named as Set-1. In similar way Set-2 is

	η/s at T=0.100 GeV	η/s at T=0.160 GeV
Upper bound [22]	0.4	0.85
Fraile et al. [8]	0.9	0.3
Lang et al. [9]	0.9	0.32
Itakura et al. [14]	1.2	0.8
Denicol et al. [18] (HRG)	1.4	0.12
Kadam et al. [19] (HRG)	1.1	0.2
Demir et al. [23] (URQMD)	1	1
Rose et al. [26] (SMASH)	1	1
Set-1 [11, 12, 22] (HRG)	0.13	0.28
Set-2 [10, 13, 22] (HRG)	0.32	0.31

	ζ/s at T=0.100 GeV	ζ/s at T=0.160 GeV
Upper bound [22]	0.13	0.38
Fraile et al. [8]	0.2	0.3
Kadam et al. [19] (HRG)	0.2	0.02
Set-1 [11, 12, 22] (HRG)	0.06	0.11
Set-2 [10, 13, 22] (HRG)	0.11	0.13

Table 1: Upper limit estimation and different model dependent estimations of η/s and ζ/s at $T = 0.100$ GeV to $T = 0.160$ GeV

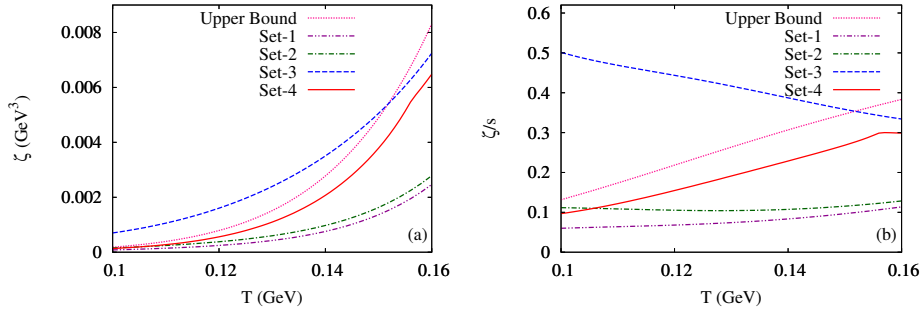


Figure 6: (Color online) The temperature dependence of (a) Bulk viscosity (ζ) (b) bulk viscosity to entropy density ratio (ζ/s) for Set-1, 2, 3, 4 and upper bound, as given in Table (2).

	Transport coefficients	Entropy density
Upper bound	$\mathcal{NR} (\tau = 10 \text{ fm}) + \mathcal{R} (\tau < 10 \text{ fm})$	$\mathcal{NR} + \mathcal{R}$
Set-1	$\mathcal{NR}^{\text{Ref. [12]}} + \mathcal{R} (\tau < 10 \text{ fm})$	"
Set-2	$\mathcal{NR}^{\text{Ref. [13]}} + \mathcal{R} (\tau < 10 \text{ fm})$	"
Set-3 ^{Ref. [22]}	$\mathcal{NR} + \mathcal{R} (\tau < 10 \text{ fm})$	„
Set-4 ^{Ref. [22]}	$\mathcal{NR} (\tau(\vec{k}) < 10 \text{ fm}) + \mathcal{R} (\tau < 10 \text{ fm})$	„

Table 2: Different set of inputs for transport coefficients (η , ζ) and entropy density (or other thermodynamical quantities like pressure, speed of sound)

created where the τ_π and τ_N results are taken from Refs. [10, 13]. Their results for η , η/s , ζ , ζ/s are shown by dash-double-dotted and dash-dotted lines in Figs. 5(a), (b), 6(a), (b). None of the curves are crossing their corresponding upper bound. It is expected because the relaxation lengths of neither \mathcal{NR} members (π and N) nor \mathcal{R} members (due to proper filtration) exceed the value of system size.

4.3 Example of using upper momentum cut-off

Let us take an example whose values of η/s and ζ/s cross our proposed upper bound. Here we will demonstrate how to consider the dissipation of hadrons within the finite size hadronic matter and how it can help to modify the values of transport coefficients within our proposed upper bound. Using the experimental values of scattering lengths for $\pi\pi$, πN , NN , KN interactions from Refs. [56, 57, 55] and πK interaction from Ref. [59, 58], their corresponding relaxation lengths have been obtained in Ref. [22]. Using the full momentum distribution of π , K and N relaxation lengths in Eqs. (6), (7) and the filtered \mathcal{R} contribution, Ref. [22] got one set of result, which is marked here as Set-3, given in Table. (2). The results of η , η/s , ζ and ζ/s are shown by blue dash line in Figs. 5(a), (b), 6(a) and (b), which are going beyond the our proposed upper bound in the low temperature domain. The reason is hidden in momentum distribution of π and K [22], where their relaxation lengths at high momentum range exceed the value 10 fm, which is assumed as the size of our system. So, we are counting some extra dissipation part, which is not at all contributing in 10 fm system size.

To resolve it, we have first track numerically the upper momentum threshold or cut-off at different temperatures for π and K , within which their relaxation lengths don't exceed the fireball dimension (10 fm). When we put those T dependent momentum thresholds as upper limit in integration of Eq. (6), (7) and use the modified results of π and K , the total values of η , η/s , ζ and ζ/s will politely go down below our proposed upper bound. This set is denotes as Set-4 in Table. (2) and the results are shown by red solid lines in Figs. 5 and 6.

Hence, our investigation states that the values of transport coefficients for hadronic matter will be within our proposed upper bound, when one will properly impose the finite size dissipation of \mathcal{NR} and \mathcal{R} components during the calculation.

So far in Sec. 4, we have deal with $R = 10$ fm system size, within which constituents are dissipating. Now if we decrease the R , then less number of \mathcal{R} members will take part in dissipation. So, considering those \mathcal{R} members and assuming R as upper relaxation lengths of \mathcal{NR} members (π , N and K), we will get R dependent of upper bound for η/s , ζ/s , as shown

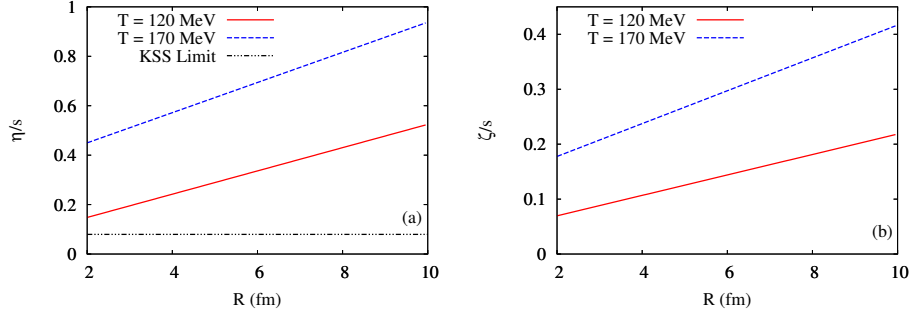


Figure 7: (Color online) Size (R) dependence of η/s (a), ζ/s (b) at $T = 0.120$ GeV and $T = 0.160$ GeV.

by red solid and blue dash lines in Fig. 7 for $T = 0.120$ GeV and $T = 0.170$ GeV respectively. We notice that reduction of system size can reduce the values of transport coefficients. In the context of fluid property, we can qualitatively conclude that η/s of smaller medium can be more close to KSS bound. It means that smaller size hadronic matter will be more close to a nearly perfect fluid behavior.

5 Conclusions and Perspectives

Present article has attempted to explore the microscopic calculations of shear and bulk viscosities for hadronic matter, where ideal hadron resonance gas model is used as a center tools. A special attention is drawn toward the finite size effect of medium, for which one may get a phenomenological upper bound of those transport coefficients. A broad numerical band, within which earlier estimated values of transport coefficients are located, can be shorten due to this finite size effect. Owing to the quantum effect, finite size can introduce a lower momentum cut-off, from where medium constituents will be distributed instead of starting from zero momentum. We have found that both the thermodynamical quantities like entropy density s , speed of sound c_s and the transport coefficients like shear viscosity η , bulk viscosity ζ can be changed when we reduce the system size lower than 6 fm.

The only dynamical input that goes in the calculation of η and ζ is the relaxation times τ of different hadrons, which are classified into resonance \mathcal{R} and non-resonance \mathcal{NR} components based on the shorter and longer lifetimes with respect to strong interaction time scale. The shorter mean life times of \mathcal{R} 's can be considered as their relaxation times. Now, for a finite size (life time) of the hadronic medium, we have to filter out those \mathcal{R} , whose relaxation length (time) cross the size (life time) of the medium. On the other hand, relaxation time of \mathcal{NR} members can be obtained from different possible scattering processes, allowed by strong interaction Lagrangian densities. Again, their relaxation length (time) should not exceed the system size (life time). Based on this phenomenological restriction, one can get an upper bound of transport coefficients. We have discussed about some sets of earlier results, where relaxation lengths of \mathcal{NR} members have not cross the system size, hence, their estimated values of transport coefficients remain within our proposed upper bound. At the end, we have taken an example, whose relaxation lengths of \mathcal{NR} members at high momentum range cross the system size. Hence, its values of transport coefficients

cross our proposed upper bound. However, by introducing an upper momentum cut-off of \mathcal{NR} members, the values of transport coefficients are reduced and gone below our proposed upper bound.

So, the current review article is desperately saying that any Hadronic model calculation of transport coefficients are different from estimation of those coefficients for 10 fm hadronic matter. Based on Refs. [22, 21], a simplified lower momentum cut-off in thermodynamical phase-space and upper momentum cut-off in relaxation length or filtering out higher decay lengths candidates are prescribed, whose outcomes are quite inclined along the phenomenological expectation of transport coefficients values. Therefore, this highly overlooked finite size effect framework should be improved towards more realistic picture and the corresponding tools should also be applied in different alternative models. It may be interesting to find the modified values of upper bound of η/s , ζ/s and its size dependence in the improved version of HRG models like excluded volume HRG (EV-HRG) models [60, 61], van der Waals (VDW) version of HRG models [62, 63].

Acknowledgements

Sabyasachi Ghosh thanks to Jayata Dey for useful help and gratefully acknowledges the contribution from his collaborators Sourav Sarkar, Bedangadas mohanty. Snigdha Ghosh acknowledges the Indian Institute of Technology Gandhinagar for the Post Doctoral Fellowship.

References

- [1] P. Kovtun, D. T. Son, and O. A. Starinets, Phys. Rev. Lett. **94**, 111601 (2005).
- [2] PHENIX collaboration, S. S. Adler et al., Phys. Rev. Lett. **91** (2003) 182301, nucl-ex/0305013; STAR collaboration, J. Adams et al., Phys. Rev. **C 72** (2005) 014904, nucl-ex/0409033.
- [3] ALICE collaboration, K. Aamodt et al., Phys. Rev. Lett. **107** (2011) 032301, nucl-ex/1105.3865; CMS collaboration, S. Chatrchyan et al., Phys. Lett. **B 724** (2013) 213–240, nucl-ex/1305.0609; ATLAS collaboration, G. Aad et al., Phys. Rev. **C 90** (2014) 024905, hep-ex/1403.0489.
- [4] J. Kinast, A. Turlapov, J.E. Thomas, Phys. Rev. Lett. **94**, 170404 (2005).
- [5] M. Muller, J. Schmalian, L. Fritz, Phys. Rev. Lett. **103**, 025301 (2009).
- [6] D. Mondal et al. Phys. Rev. Lett. **118**, 192501 (2017).
- [7] A. Dobado and S.N. Santalla, Phys. Rev. **D 65**, 096011 (2002); A. Dobado and F. J. Llanes-Estrada, Phys. Rev. **D 69**, 116004 (2004).
- [8] D. Fernandez-Fraile and A. Gomez Nicola, Eur. Phys. J. **C 62**, 37 (2009).
- [9] R. Lang, N. Kaiser and W. Weise Eur. Phys. J. **A 48**, 109 (2012).
- [10] S. Mitra, S. Ghosh, and S. Sarkar Phys. Rev. **C 85**, 064917 (2012).
- [11] S. Ghosh, G. Krein, S. Sarkar, Phys. Rev. **C 89**, 045201 (2014).

- [12] S. Ghosh, Phys. Rev. **C 90** 025202 (2014); S. Ghosh, Braz. J. Phys. 45 (2015) 687.
- [13] U. Gangopadhyaya, S. Ghosh, S. Sarkar, S. Mitra. Phys. Rev. **C 94**, 044914 (2016).
- [14] K. Itakura, O. Morimatsu, and H. Otomo, Phys. Rev. **D 77**, 014014 (2008).
- [15] M. Prakash, M. Prakash, R. Venugopalan, and G. Welke, Phys. Rep. **227**, 321 (1993).
- [16] M. I. Gorenstein, M. Hauer, O. N. Moroz, Phys. Rev. **C 77**, 024911 (2008).
- [17] J. Noronha-Hostler, J. Noronha, C. Greiner, Phys. Rev. Lett. **103**, 172302 (2009).
- [18] G. S. Denicol, C. Gale, S. Jeon, and J. Noronha, Phys. Rev. **C 88**, 064901 (2013).
- [19] G. P. Kadam and H. Mishra, Phys. Rev. **C 92**, 035203 (2015).
- [20] G. P. Kadam and H. Mishra, Nucl. Phys. **A 934**, 133 (2015).
- [21] S. Samanta, S. Ghosh, B. Mohanty, J. Phys. **G 45**, 075101 (2018).
- [22] S. Ghosh, S. Ghosh, S. Bhattacharyya, Phys. Rev. **C 98**, 045202 (2018).
- [23] N. Demir and S.A. Bass Phys. Rev. Lett. 102, 172302 (2009).
- [24] A. Muronga, Phys. Rev. **C 69**, 044901 (2004).
- [25] S. Pal, Phys. Lett. **B 684** (2010) 211.
- [26] J.-B. Rose, J. M. Torres-Rincon, A. Schäfer, D. R. Oliinychenko and H. Petersen, Phys. Rev. C **97**, no. 5, 055204 (2018)
- [27] A. Dobado, F.J.Llane-Estrada, J. Torres Rincon, Phys. Lett. **B 702**, 43 (2011).
- [28] A. Dobado, J. Torres Rincon, Phys. Rev. **D 86**, 074021 (2012).
- [29] D. Fernandez-Fraile and A. Gomez Nicola, Phys. Rev. Lett. **102**, 121601 (2009).
- [30] S. Mitra and S. Sarkar, Phys. Rev. **D 87**, 094026 (2013); S. Mitra, U. Gangopadhyaya, and S. Sarkar, Phys. Rev. **D 91**, 094012 (2015).
- [31] S. Ghosh, S. Chatterjee, B. Mohanty Phys. Rev. **C 94** (2016) 045208.
- [32] G. Sarwar, S. Chatterjee, Jane Alam, J. Phys. G 44 (2017) 055101.
- [33] P. Chakraborty and J. I. Kapusta, Phys. Rev. C **83**, 014906 (2011).
- [34] S. Gavin, Nucl. Phys. **A, 435**, 826 (1985).
- [35] S. Ghosh, Int. J. Mod. Phys. A **29**, 1450054 (2014).
- [36] P. Braun-Munzinger, K. Redlich, J. Stachel, Quark Gluon Plasma 3, eds. R.C. Hwa and X.N. Wang, (World Scientific Publishing, 2004), nucl-th/0304013.
- [37] S. Borsanyi, Z. Fodor, C. Hoelbling, S. D. Katz, S. Krieg and K. K. Szabo, Phys. Lett. B **730**, 99 (2014)
- [38] A. Bazavov *et al.* [HotQCD Collaboration], Phys. Rev. D **90**, 094503 (2014)

- [39] M. Lüscher, Commun. Math. Phys. **104**, 177 (1986).
- [40] J. Gasser and H. Leutwyler, Phys. Lett. B **188**, 477 (1987).
- [41] C. Spieles, H. Stoecker and C. Greiner, Phys. Rev. C **57**, 908 (1998).
- [42] A. Gopie and M. C. Ogilvie, Phys. Rev. D **59**, 034009 (1999).
- [43] L. M. Abreu, M. Gomes and A. J. da Silva, Phys. Lett. B **642**, 551 (2006).
- [44] J. Luecker, C. S. Fischer and R. Williams, Phys. Rev. D **81**, 094005 (2010).
- [45] E. S. Fraga, L. F. Palhares and P. Sorensen, Phys. Rev. C **84**, 011903 (2011).
- [46] A. Bhattacharyya, R. Ray, S. Samanta and S. Sur, Phys. Rev. C **91**, no. 4, 041901 (R) (2015).
- [47] A. Bhattacharyya, S. K. Ghosh, R. Ray, K. Saha and S. Upadhaya, Europhys. Lett. **116**, no. 5, 52001 (2016).
- [48] N. Magdy, M. Csanád and R. A. Lacey, J. Phys. G **44**, no. 2, 025101 (2017).
- [49] K. Redlich and K. Zalewski, arXiv:1611.03746 [nucl-th].
- [50] F. Karsch, K. Morita, K. Redlich, Phys. Rev. C **93**, 034907 (2016).
- [51] K. Saha, S. Ghosh, S. Upadhaya, S. Maity, Phys. Rev. D **97** (2018) 116020.
- [52] L. Adamczyk et al. (STAR Collaboration), Phys. Rev. C **96**, 044904 (2017).
- [53] V. Roy, A. K. Chaudhuri and B. Mohanty, Phys. Rev. C **86**, 014902 (2012).
- [54] C. Patrignani et al. (Particle Data Group), Chin. Phys. C, 40, 100001 (2016).
- [55] M. Fukugita, Y. Kuramashi, M. Okawa, H. Mino, A. Ukawa, Phys. Rev. D **52**, 3003 (1995).
- [56] M. M. Nagels et al. , Nucl. Phys. B **147**, 189 (1979)
- [57] O. Dumbrajs et al. , Nucl. Phys. B **216**, 277 (1983).
- [58] N. T. Xiem, S. Shinmura, Prog. Theor. Exp. Phys. 2014, 023D04 (2014).
- [59] P. Buttiker, S. Descotes-Genon, and B. Moussallam, Eur. Phys. J. C **33**, 409 (2004).
- [60] D. H. Rischke, M. I. Gorenstein, H. Stoecker, W. Greiner, Z. Phys. C 51, 485 (1991).
- [61] P. Braun-Munzinger, I. Heppe, and J. Stachel, Phys. Lett. B 465, 15 (1999).
- [62] V. Vovchenko, M. I. Gorenstein and H. Stoecker, Phys. Rev. Lett. 118, 182301 (2017).
- [63] S. Samanta and B. Mohanty, Phys. Rev. C 97, 015201 (2018).